Available online at www.sciencedirect.com
ScienceDirect
Microelectronic Engineering 84 (2007) 151–160
MICROELECTRONIC ENGINEERING
www.elsevier.com/locate/mee

Enhancing the reliability of n^{+}–p junction diodes using plasma treated tantalum barrier film

Keng-Liang Ou [a,*], Wen-Fa Wu [b], Shi-Yung Chiou [c]

[a] Graduate Institute of Oral Sciences, College of Oral Medicine, Taipei Medical University, Taipei 110, Taiwan, ROC
[b] National Nano Device Laboratories, Hsinchu 300, Taiwan, ROC
[c] Department of Mold and Die Engineering, National Kaohsiung University of Applied Sciences, Kaohsiung 807, Taiwan, ROC

Received 29 November 2005; received in revised form 9 September 2006; accepted 25 September 2006
Available online 20 October 2006

Abstract

The properties of Ta barrier films treated with various plasma nitridations have been investigated by Cu/barrier/Si. An amorphous layer is formed on Ta barrier film after plasma treatments. The thickness of the amorphous layer is about 3 nm. Plasma treated Ta films possess better barrier performance than sputtered Ta and TaN films. It is attributed to the formation of a new amorphous layer on Ta surface after the plasma treatment. Cu/Ta(N,H)/Ta (10 nm)/Si remained stable after annealing at 750 °C. Ta(N,H)/Ta possesses the best thermal stability and excellent electrical properties. Cu/Ta/n^{+}–p and Cu/Ta(N,O)/Ta/n^{+}–p diodes resulted in large reverse-bias junction leakage current after annealing at 500 °C and 600 °C, respectively. On the other hand, Ta(N,H)/Ta and Ta(N)/Ta diffusion barriers improve the thermal stability of junction diodes to 650 °C. Ta(N,H)/Ta barrier film possesses lowest resistivity among Ta, Ta(N,O)/Ta, and Ta(N)/Ta films. Hydrogen plays an important role in enhancement of barrier properties. It is believed that hydrogen not only induces amorphization on Ta, but also eliminates the oxygen in the film. It is believed that the enhancement of ability against the copper diffusion is due to the combined effects of the hydrogen reaction and nitridation.
© 2006 Elsevier B.V. All rights reserved.

Keywords: Copper; Tantalum; Amorphization; Hydrogen

1. Introduction

Copper is an attractive material for interconnection due to its lower electrical resistivity and better electromigration resistance compared to Al-based alloys. Cu is considered for application in integrated circuits. However, it is well known that copper diffuses quickly in Si and SiO_2 [1,2], which causes degradation of transistor reliability by forming particular impurity levels. Because of its ability to rapidly diffuse in silicon and degrade reliability, the development of effective diffusion barrier materials is the most important issue for the realization of Cu interconnection in Si-based integrated circuits [3,4]. Many materials were used as a diffusion barrier in copper metallization technique. Refractory metals and their nitrides had been investigated for such applications [5–12]. Among them, tantalum and tantalum nitride have drawn the most attention owing to their high thermal stability and resistance to form compounds with copper. Previous studies have shown that TaN is more desirable than Ta in terms of barrier effectiveness. However, resistivity of tantalum nitride film is higher than that of tantalum film [11,12]. Recently, multilayered TiN/Ti and TaN/Ta barriers as the best barrier for copper metallization were investigated by many researchers [13–15]. As the technology node move to 0.18 μm and below, a thin barrier layer is necessary to lower the resistance of the total line interconnect and/or via. It becomes probably inappropriate to use a multilayered barrier thicker than 30 nm, and hence investigations of the thermal stability and barrier properties of ultrathin barrier layers in the Cu metallization system are important [13,14,16–20]. In paral-

* Tel.: +886 3 27361661x5400; fax: +886 3 27362295.
E-mail address: klou@tmu.edu.tw (K.-L. Ou).

0167-9317/$ - see front matter © 2006 Elsevier B.V. All rights reserved.
doi:10.1016/j.mee.2006.09.021

lel with the development of technology, the sizes of node move to 0.18 μm and below, a thin barrier layer is necessary to lower the resistance of the total line interconnect and/or via. It becomes inappropriate to use a barrier thicker than 30 nm, and hence investigations of the thermal stability and barrier properties of ultra-thin barrier layers in the Cu metallization system are crucial.

In the present research, the barrier properties and thermal stability of ultra-thin Ta-based barrier layers (10 nm) in the Cu metallization system were studied. Furthermore, a new method to form nitrogen and oxygen incorporated Ta films with low resistivity and high thermal stability were investigated. N_2, N_2O and NH_3 plasmas were used to post-treat the Ta barrier films. Properties of barrier films were evaluated by material analyses and electrical measurements.

2. Experimental details

The Cu/Ta/n^+–p, Cu/TaN/n^+–p, Cu/Ta(N)/Ta/n^+–p, Cu/Ta(N,O)/Ta/n^+–p, and Cu/Ta(N,H)/Ta/n^+–p junction diodes were fabricated for barrier capability of Ta and Ta with various plasma treatment. The substrates used in the present experiments were 6-in., p-type (100) oriented Si wafers with nominal resistivity of 5–10 Ω-cm. The Si wafers were cleaned in a dilute HF solution (HF:H_2O = 1:50) for 10 min, and rinsed in de-ionized water. After RCA standard cleaning, the wafers were thermally oxidized at 1050 °C in steam atmosphere to grow a 500 nm oxide layer. Diffusion regions with areas $500 \times 500\ \mu m^2$ and $1000 \times 1000\ \mu m^2$ were defined on the oxide-covered wafers using the conventional photolithographic technique. The n^+–p junctions with junction depths of 0.3 μm were formed by BF_2^+ implantation at 40 keV to a dose of $5 \times 10^{15}\ cm^{-2}$ followed by furnace annealing at 900 °C for 30 min in N_2 ambient. After the junctions were formed, the wafers were prepared for deposition of Ta and TaN barrier layer. Ta and TaN films were deposited with a 6-in. diameter Ta target in an Ar and Ar + N_2 atmosphere by a magnetron sputtering system, respectively. The sputtering system was evacuated using a dry pumping system to reach a base pressure of 6.67×10^{-5} Pa. The sputtering pressure and power were 0.8 Pa and 500 W, respectively. Some wafers were further received ex-situ N_2, N_2O and NH_3 plasma treatments in a plasma enhanced chemical vapor deposition (PECVD) system after deposition of Ta films. In addition, TaN (10 nm) films were also deposited by reactive sputtering for comparison. They were prepared using optimum conditions in previous investigations, provided a better barrier capability against Cu diffusion [11]. For the purpose of easy identification, the sputtered tantalum, tantalum nitride, N_2, N_2O and NH_3 plasma treated tantalum films were denoted as Ta, TaN, Ta(N)/Ta, Ta(N,O)/Ta and Ta(N,H)/Ta, respectively. Copper films with a thickness of 300 nm were deposited on the barrier metal using the same sputtering system. During sputtering, gas pressure was maintained at 0.8 Pa with a power selected at 1500 W. Finally, Cu patterns were defined and etched using dilute (5 vol%) HNO_3, while Ta, TaN and Ta with plasma treatment were etched using SF_6/N_2 plasma for the preparation of Cu/Ta/n^+–p, Cu/TaN/n^+–p, and Cu/plasma treated Ta/n^+–p. The schematic cross sections of these differently metallized n^+–p junction diodes are illustrated in Fig. 1. To evaluate the thermal stability, Cu/Ta/Si, Cu/TaN/Si, Cu/Ta(N)/Ta/Si, Cu/Ta(N,O)/Ta/Si, and Cu/Ta(N,H)/Ta/Si were annealed in vacuum from 500 °C to 800 °C for 1 h. The vacuum level is 1.33 Pa. Surface morphologies of the barrier films were analyzed by a Nanoscope III atomic force microscope (AFM) with a Si probe. AFM probe was scanned over an area of $5 \times 5\ \mu m^2$ with 512 scans at 1 Hz scanning rate in tapping mode. Sheet resistance measurements were taken using a four-point probe system. The compositions of the films were analyzed by X-ray photoemission spectroscopy (XPS) with a monochcromatic Mg Kα source. The X-ray power was 250 W (15 kV at 16.7 mA). The XPS energy scale was calibrated by setting the binding energy of $Ag_{3d_{5/2}}$ line on clean silver to exactly 368.3 eV referenced to the Femi level. The angle of incidence of the X-ray beam with the specimen normal was 45°. High-resolution scans were run for Ta and N using an X-ray beam with about a 15 nm diam. In addition, X-ray photoelectron spectroscopy (XPS) using monochromatized Mg Kα radiation was performed to identify the chemical states of tantalum films with various plasma treatments. Auger electron microscopy (AES) using the primary electron energy of 5 keV and modulation voltage of 4 V. The sputter etching of the sample surface by 3 keV Ar ion was made before obtained an AES spectrum. In order to realize the capability of barrier layer against copper diffusion, grazing incidence X-ray diffractometry (GIXRD) was carried out for phase identification. The incident angle of X-ray was fixed at three degrees. X-ray diffractometer with Cu Kα radiation operated at 50 kV and 250 mA. Microstructure variations were investigated by transmission electron microscopy (TEM). Plan-view TEM samples were prepared electron transparency by mechanical thinning followed by ion milling in a preci-

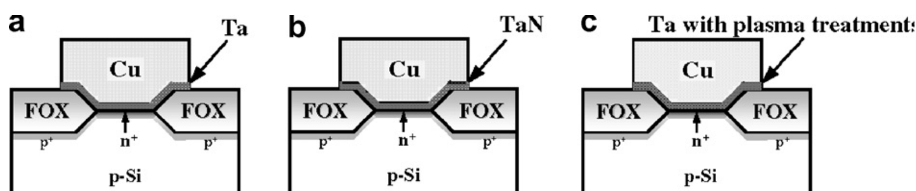

Fig. 1. Schematic diagram of Cu/barrier/n^+–p junction diodes used in this study.

sion ion polishing system (PIPS). A Hitachi H9000NAR TEM system operating at an acceleration voltage of 300 kV was used for observation of TEM and HRTEM images and nanoprobe electron diffraction. The Rutherfold backscattering spectroscopy (RBS) was carried out by using 2 MeV He^{2+} beam with backscattered angle of 20°. The elemental compositions of the Ta and Ta with plasma treatments were obtained from RBS data using standard RUMP analysis. For electrical analyses, Leakage current of the diodes was measured by HP4145B semiconductor parameter-analyzer at a reverse-bias of −5 V. After annealing at various temperatures for 1 h, the diode leakage current was measured.

3. Results and discussion

Fig. 2 shows the X-ray diffraction spectra of Ta(N,H)/Ta film. The intensity and shape of reflections indicate microstructure variations of Ta films. As-deposited Ta films grow predominantly in bcc-Ta phase and are apparently polycrystalline. The increase of nitrogen concentration after 5-min plasma treatment results in intensification and the shape of reflections of β-Ta(N) phase with tetragonal structure decrease obviously. By further 30-min plasma treatment, the broadening of the peak is obvious, but the crystalline structure is preserved. Ta(N)/Ta and Ta(N,O)/Ta films have the same results by GIXRD analysis. To further determine the structure variations of the barrier films with various plasma treatments, the films were analyzed using plan-view TEM. Fig. 3 shows series of bright field images (BF) and selected area diffraction patterns (SADP) of the Ta films following various NH_3 plasma treatment time. The BF image and SADP of the Ta film clearly show that the film is bcc-Ta with grain size 20–30 nm, as shown in Fig. 3(a). Based on the results, it is concluded that as-deposited Ta film with bcc structure and (1 1 0) texture. Fig. 3(b) shows the BF image and SADP of the Ta(N,H)/Ta film after 5-min plasma treatment. It clearly shows that the films contains β-Ta(N) and bcc-Ta phases and the grain size of the this film is similar to as-deposited Ta film. Fig. 3(c) shows both the TEM image and SADP of Ta(N,H)/Ta film after 30-plasma treatment. It is obvious that the film forms an amorphous-like struc-

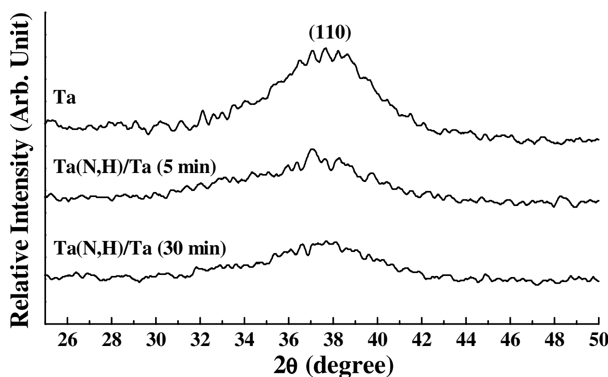

Fig. 2. GIXRD spectra of Ta films with NH_3 plasma treatment.

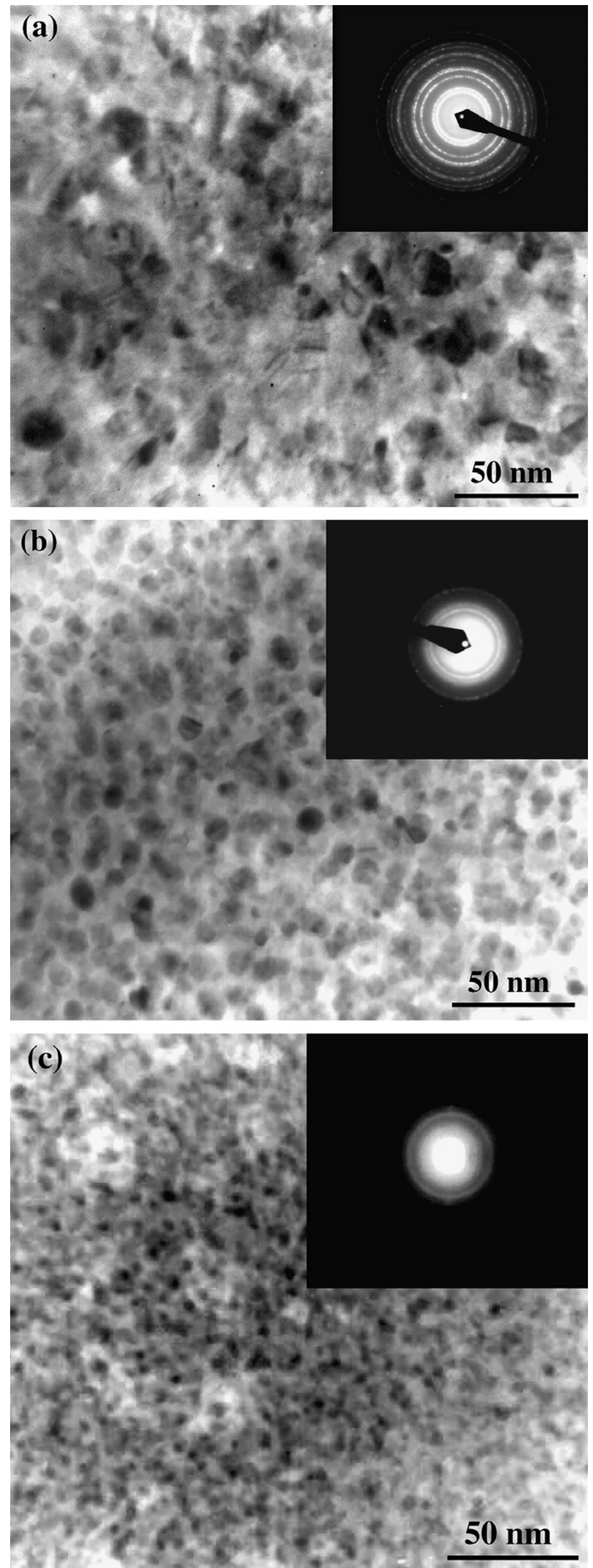

Fig. 3. Plan-view TEM micrographs and selected area diffraction patterns of Ta film with NH_3 plasma treatments; (a) without treatment, (b) 5 min, (c) 30 min.

ture. The small nitrogen addition would result in the phase transformation from bcc-Ta to bct-Ta(N). Moreover, it is quite well established that sputtered Ta films with N, C, or O impurities tend to form tetragonal structures due to the incorporation of impurities into interstitial potions [11]. An amorphous-like layer is formed after 30-min plasma treatment and the nitrogen content is about 42 at.%, detecting by RBS. Ta_2N phase was formed as nitrogen concentration is between about 20 and 50 at.%, but an amorphous component also appears in the this nitrogen range [12]. Furthermore, it is obvious that as plasma treated time increases, the peak shapes become broad gradually for the (1 1 0) peak corresponding to bct-Ta(N) phase. The phenomenon indicates lattice distortion and /or development of an amorphous-like Ta(N) thin film after plasma treatments. Fig. 4 shows N 1s X-ray photoelectron spectra of Ta films after various plasma treatments of 30 min. Chemical bonding states corresponding to nitrogen are observed duration of N_2 and NH_3 plasma treatment, as shown in Fig. 4. The position of the N 1s level is clearly shifting corresponded to N 1s (398.1 eV) after N_2 and NH_3 plasma treatments. The peak at ~401 eV is ascribed to the nitrogen atoms or molecules present in interstitial sites. This kind of nitrogen is also detected in tungsten nitride film prepared by the reduction of WF_6 and N_2 gas [10]. As the N_2 plasma treatment time increased up to 30 min, the emission peak at ~401 eV is dominated in the N 1s spectrum. These results indicate that some N atoms do not form strong covalent or ionic bonds with Ta atoms during the plasma nitridation of Ta film. Some of the introduced N atoms segregate at the interstitial sites and grain boundaries in the tantalum film as impurities. Similar results were observed in preparing chemical vapor deposited tungsten nitride film [13]. It is believed that Ta–N bonding is formed after nitrogen-containing plasma treatments. However, N 1s peak is not distinctly observed obviously in Ta(N,O) barrier film after N_2O plasma treatment. On the other hand, tantalum and oxygen bonding was obviously detected in Ta(N,O) film by XPS analysis, and the position of the O 1s level is located at ~534 eV, shown in Fig. 5. It is clearly shifted corresponding to O 1s (531 eV). It is believed that Ta–O bonding is formed after bombardment of the oxygen ions and radicals. In order to understand the nitridation and oxygen effect, distribution of oxygen and nitrogen were analyzed by Auger electron spectroscopy. The spectra obtained are presented in Fig. 6. Fig. 6(a) shows the oxygen content was detected on the surface of tantalum film and nitrogen content was not observed on as-deposited Ta film. It is interpreted that a thin tantalum oxide was formed on tantalum surface. The depth profile of the Ta(N)/Ta film (Fig. 6(b)) shows that nitrogen has diffused into tantalum surface and the composition is $Ta_{2.0}N_1$ as confirmed by RBS analysis. Fig. 6(c) shows the variation of oxygen–nitrogen profiles on Ta(N,O) film after N_2O plasma treatment. It shows that the tantalum reaction proceeds through surface oxidation. It seems that oxidation occurs mainly at the beginning of the treatment; oxygen is thought to be incorporated during plasma treatment. For short plasma treated duration, oxidation of tantalum predominates through rapid oxygen diffusion into the film. As plasma treated duration is long enough, nitrogen starts to react with the partially oxidized tantalum at the surface; nitrogen is incorporated into the oxidized region whereas oxygen is rejected. However, the oxygen species was also bombarded on tantalum film in N_2O plasma treatment. In the deeper part of the film, and up to the interface, the metal is oxidized. In Fig. 6(d), in the deeper surface region the nitrogen content is higher whereas oxygen content is a little after tantalum film with NH_3 plasma treatment. This can be interpreted by a reaction of nitriding species with oxidized tantalum that results in an exchange between nitrogen and oxygen in surface and hydrogen play an important role in the reaction. Normalized resistivity of 10 nm Ta(N)/Ta, Ta(N,H)/Ta and Ta(N,O)/Ta films before and after plasma treatments was shown in Fig. 7. As plasma treated duration increases from 5 to 15 min, the resistivity decreases initially and then increases ultimately. However, resistivity of 30-min plasma treated tantalum film does not increase further. It is believed that densification effects could occur due to

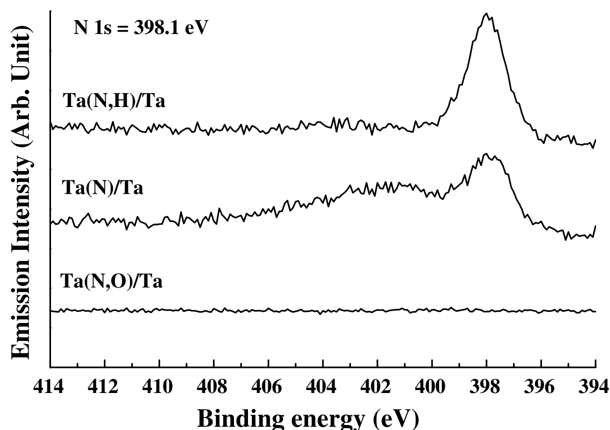

Fig. 4. N 1s XPS spectra of Ta films after various plasma treatments for 30 min.

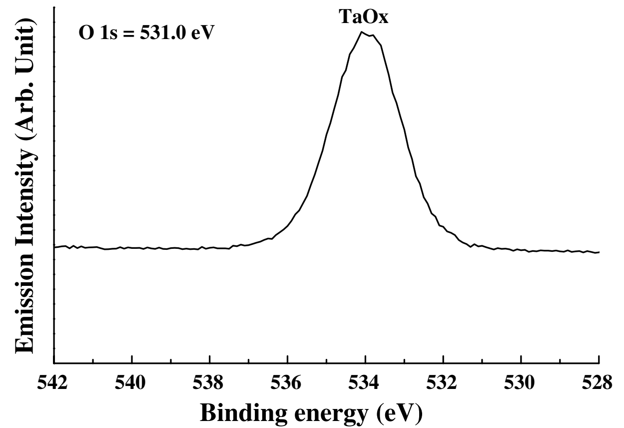

Fig. 5. O 1s XPS spectrum of Ta films before and after N_2O plasma treatment.

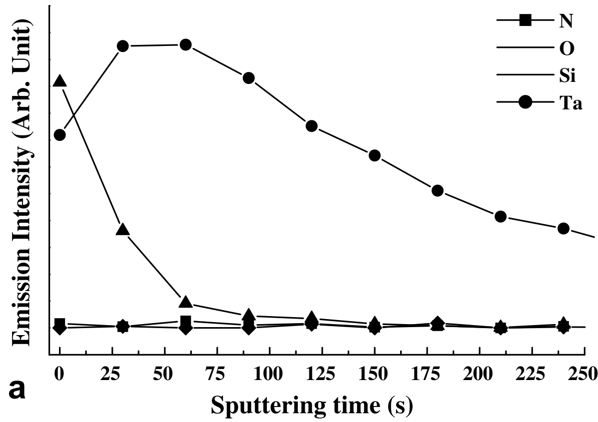

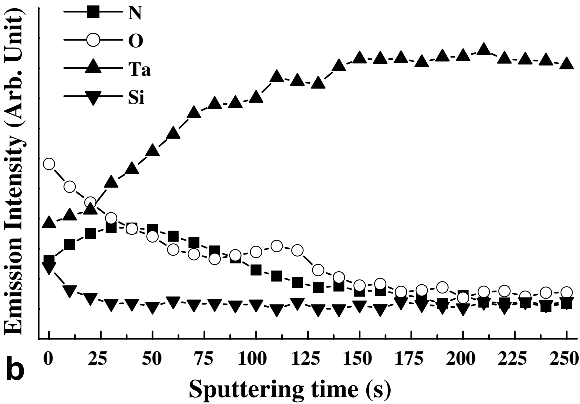

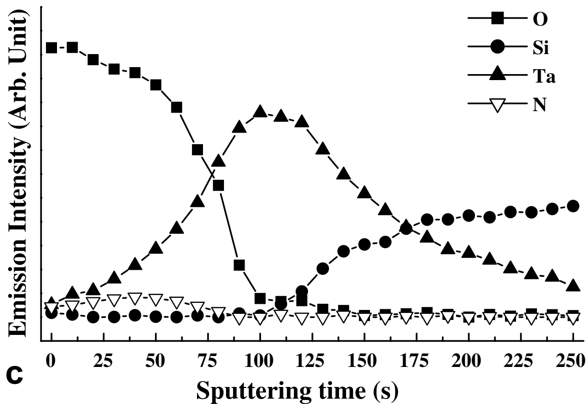

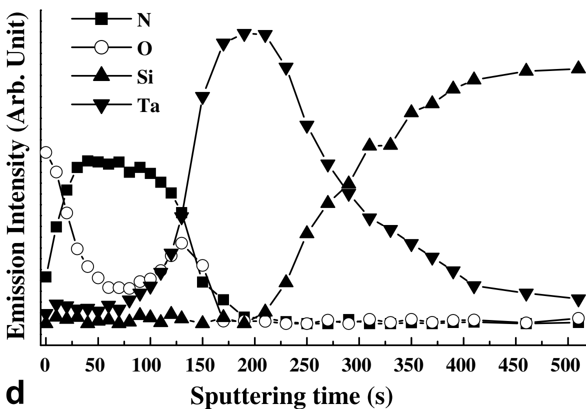

Fig. 6. AES profiles of plasma treated Ta film; (a) Ta, (b) Ta(N)/Ta, (c) Ta(N,O)/Ta, (d) Ta(N,H)/Ta.

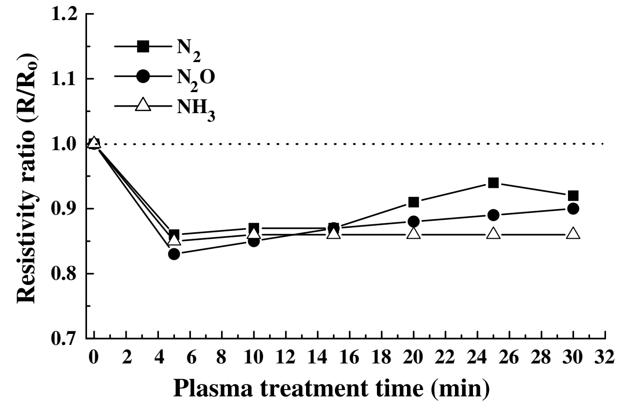

Fig. 7. Normalized resistivity of Ta films (10 nm) after various plasma treatments with various durations.

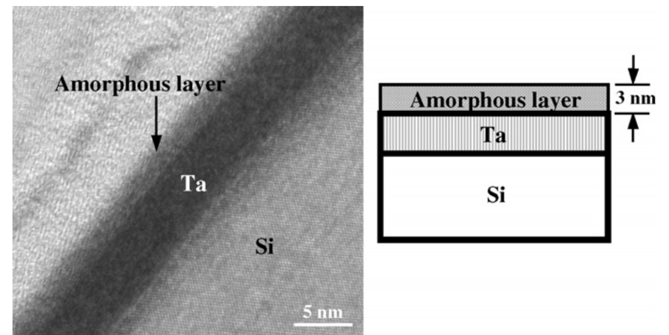

Fig. 8. Cross-sectional TEM micrograph of Ta(N,H)/Ta/Si.

the bombardments of energetic ions and radicals. The improvement in the density of the film would result in the enhancement in conductivity of the film. Fig. 8 shows that the cross-sectional TEM images of Ta film with 30-min NH_3 plasma treatment. The thickness of the amorphous layer is above 3 nm. The development of an amorphous-like Ta(N,H) layer on the film surface was observed. However, there is also something below the Ta layer with similar appearance. Further, based on the AES result, as shown in Fig. 6(d), this could be native oxygen containing layer. The formation of the amorphous-like layer would increase the resistivity due to increasing scattering effects. It is believed that the variation in resistivity is due to the combined effects as mentioned above. The densification effects are the dominant factor in the early plasma treatment, and resistivity would increase corresponding to the development of the amorphous layer after increasing plasma treatments. In order to realize the densification effects after plasma treatments, densities of Ta films following various plasma treatments are evaluated by RBS and shown in Fig. 9. The theoretical densities (bulk densities) of Ta and TaN are also shown in Fig. 9. The density of Ta(N,O)/Ta film is 5.82 g/cm^3. It appears to be much lower than that of bulk TaN(16.3 g/cm^3) and Ta (16.6 g/cm^3). The densities of Ta(N)/Ta and Ta(N,H)/Ta films are 14.7 g/cm^3 and 15.93 g/cm^3, respectively. It is pointed out that the densification of the amorphous-like

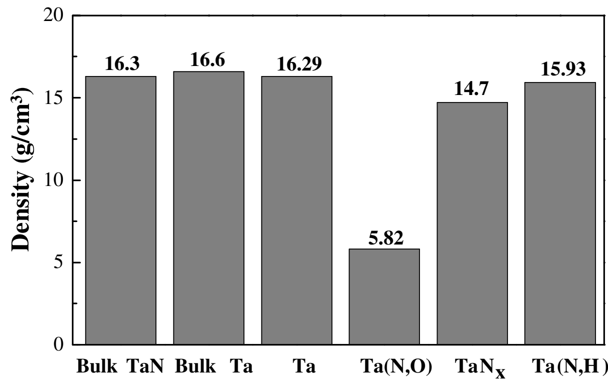

Fig. 9. Density of Ta and TaN with and without various plasma treatments.

films formed on Ta surface is quite different from that of bulk TaN. In other words, the existence of excess light elements results in much lower gram densities relative to that of bulk TaN and Ta. Ta(N,O)/Ta film has lower effective resistivity and low density (~160.2 μΩ-cm, 5.82 g/cm^3) than the as-deposited Ta film (~178 μΩ-cm, 16.29 g/cm^3). On the other hand, the films treated by N_2 and NH_3 plasma treatment also have low resistivity of the films (~163.76 μΩ-cm, 149.52 μΩ-cm) and film densities increase (Ta(N)/Ta = 14.7 g/cm^3 and Ta(N,H)/Ta = 15.93 g/cm^3). Based on the above investigation, the amorphous-like layer induced by plasma treatment possesses lower resistivity and high density and the Ta(N,H)/Ta film possesses highest densification effect than any other post-treatments. It is due to the fact that NH_3 gas has lower decomposition energy and tends to decompose into hydrogen and nitrogen ions, which interact with Ta films. Fig. 10 shows surface roughness of Ta films with and without plasma treatment. It can be seen that the longer durations of plasma treatments are, the smoother the surface roughness are. It revealed that energetic radical and/or ion reactions could resputter the tantalum film and make the film smoother. Resultant roughness is consistent with the GIXRD and TEM results. That is, the microstructures of Ta films transforms from columnar polycrystal to nanocrystal after plasma treatments. Ta(N,O)/Ta film has largest surface

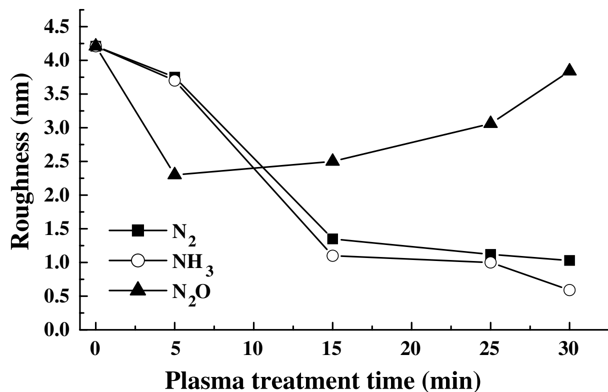

Fig. 10. Surface roughness of Ta thin films as a function of plasma treatment time.

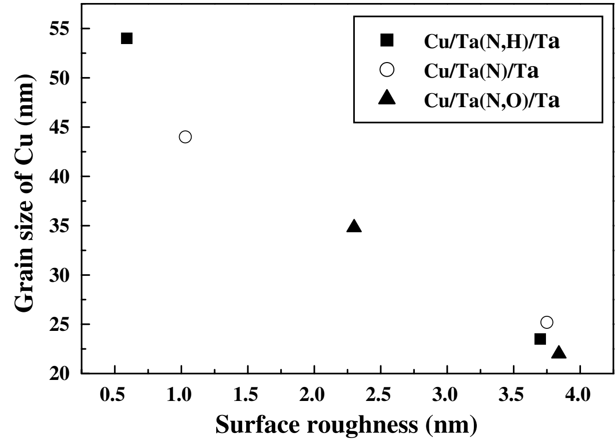

Fig. 11. Correlation between surface roughness and grain size of Cu film.

roughness than any other treated films. It revealed that ion bombardment effect of oxygen ions and radicals is stronger than that of nitrogen. Preferred orientations of the Cu films on the plasma treated barrier layers were demonstrated by GIXRD analysis. Fig. 11 shows the surface roughness of Cu films after deposited on Ta film with various plasma treatments. It is obvious that deposited Cu film on Ta(N,O) film possesses higher surface roughness and smaller grain sizes. It revealed that heavier oxygen ions bombarded on Ta surface and induced a rougher surface. There are more nucleation sites, thereby resulting formation of small grains. This phenomenon is also observed in electroplated Cu interconnection [14].

Fig. 12 shows the variations in sheet resistance of Cu/barrier/Si after annealing at various temperatures. The variation in the sheet resistance is designated as the ratio of (R–R_0) to R_0, which R_0 and R denote the sheet resistance of as-deposited sample and R is the sheet resistance of the annealed sample, respectively. The result reflects interactions between layers. It is noted that the sheet resistance initially decreases by even annealing at 500 °C, which apparently is caused by a decrease in defect density and

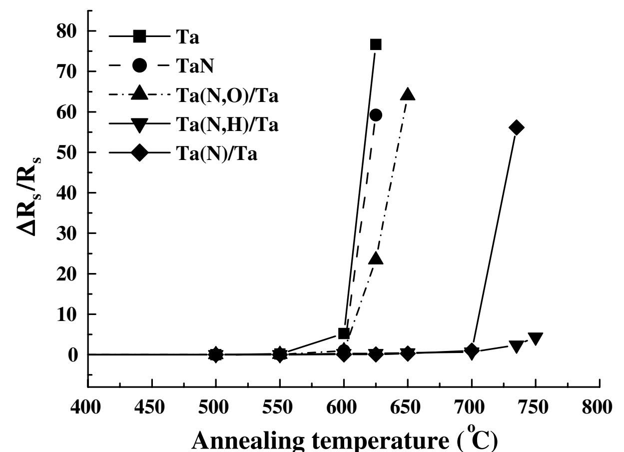

Fig. 12. Variation of sheet resistance for Cu/barriers/Si as a function of annealing temperature.

grain growth in the Cu film. The sheet resistance of the Cu/Ta/Si film increased slightly upon annealing at 600 °C. However, after annealing at 625 °C, the appearance of the sample becomes gray and the sheet resistance of the sample drastically increases, indicating that a significant reaction has now occurred between the layers. A similar behavior was observed at 625 °C, 650 °C and 750 °C for Cu/TaN/Si Cu/Ta(N,O)/Ta/Si and Cu/Ta(N)/Ta/Si, respectively, while the observations for the Cu/Ta(N,H)/Ta/Si samples were unremarkable even after annealing at 750 °C. The result confirms no compound formation between Cu and Si. It is obvious that Ta barrier films with post-treatment possesses higher thermal stability than as-sputtered Ta and TaN barrier film and NH_3 plasma treated Ta barrier film possesses the best thermal stability. Fig. 13 shows XRD spectra of Cu/barrier/Si without and with various plasma treatments by various annealing temperatures. Fig. 13(a) shows the XRD spectra for Cu/Ta/Si samples

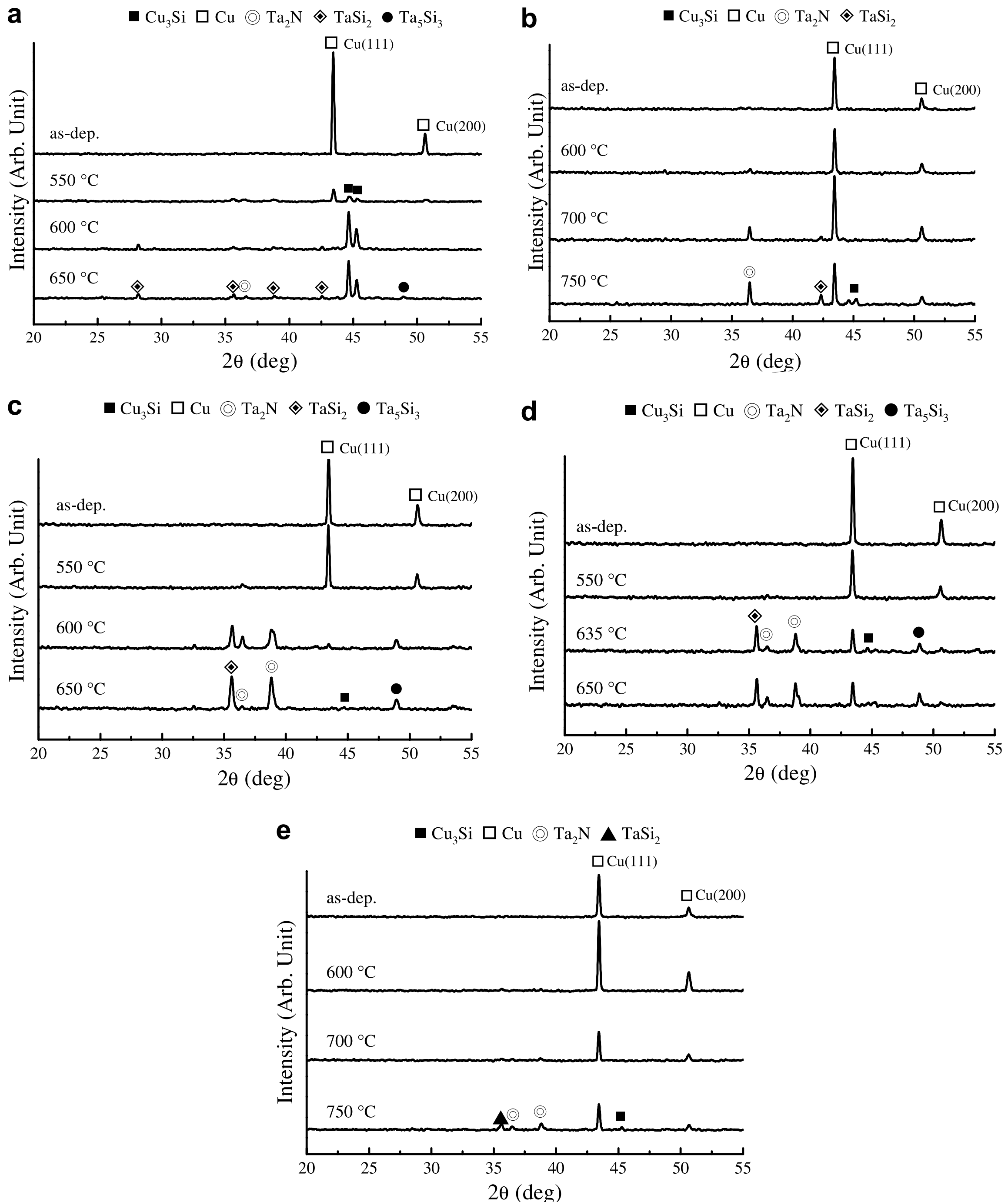

Fig. 13. XRD spectra of Cu/plasma treated Ta/Si before and after annealing for various temperatures; (a) as-sputtered Ta, (b) 30-min N_2 plasma treated Ta, (c) 30-min N_2O plasma treated Ta, (d) 5-min NH_3 plasma treated Ta, (e) 30-min NH_3 plasma treated Ta.

subjected to annealing at various temperatures. Strong Cu(1 1 1) and weak Cu(2 0 0) peaks were observed in all annealed samples, indicating that the Cu had preferential ⟨1 1 1⟩ crystal orientation. It had been reported that Cu with high ⟨1 1 1⟩ texture provided higher electromigration resistance [2]. For the Cu/Ta/Si sample annealed at 550 °C, $TaSi_2$ and Cu_3Si phases were detected, indicating the failure of the Ta barrier layer. The high-resistivity Cu_3Si formation and related Cu decrease resulted in the great increase of sheet resistance as shown in Fig. 12. XRD results for Cu/Ta(N)/Ta/Si samples show that the crystallization of amorphous-like Ta(N) layer occurs after annealing at 600 °C. As shown in Fig. 13(b), Ta_2N and $TaSi_2$ phases were detected after annealing at temperatures, 600 °C and 700 °C, respectively. After annealing at 750 °C for 1 h, peaks of Cu_3Si were detected. In respect of the formation of tantalum silicide, the formation temperature of the sample with Ta(N)/Ta barrier was higher than that of

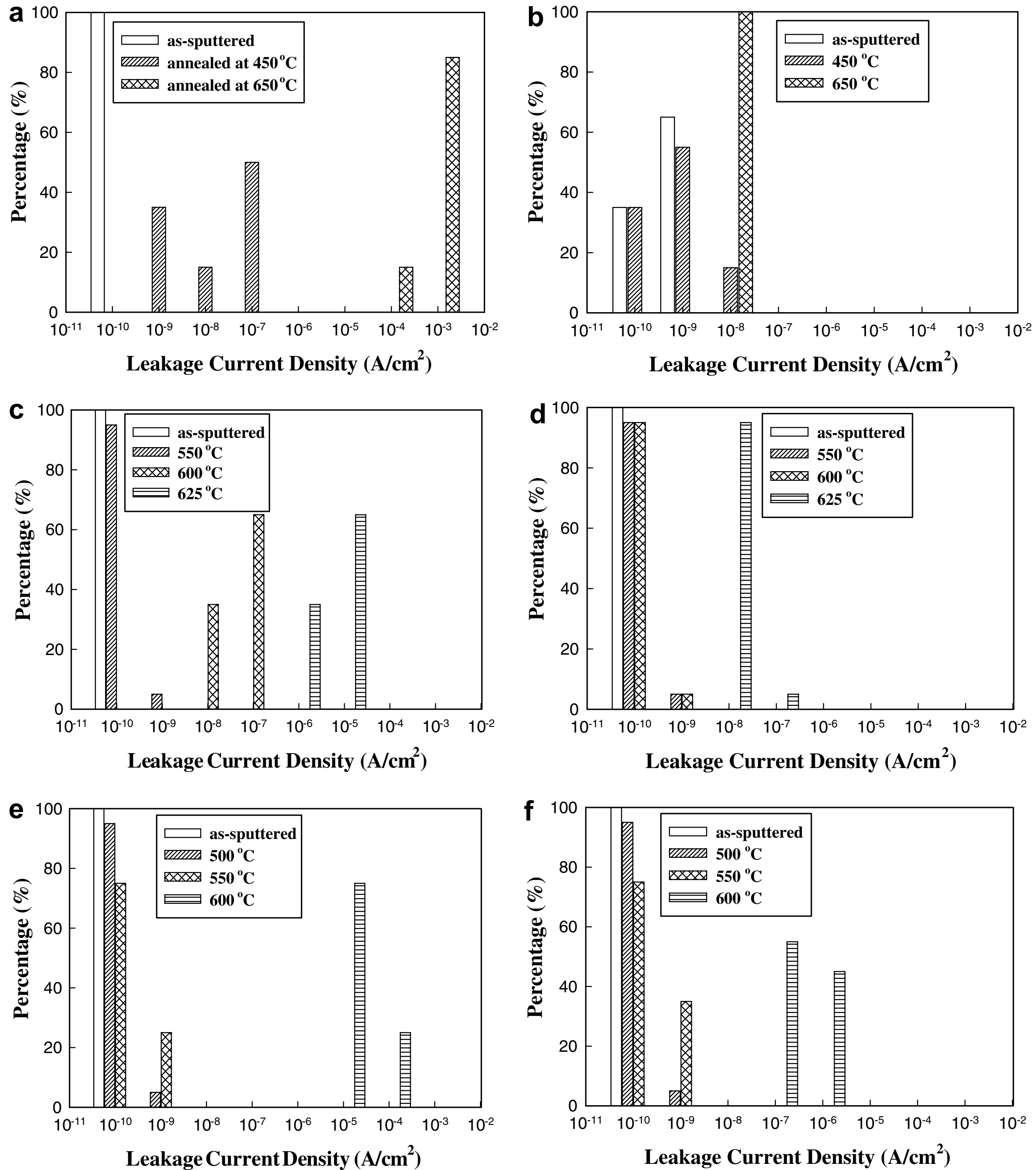

Fig. 14. n⁺–p Diode leakage current density distribution of the (a) Cu/Ta(10 nm)/Si, (b) Cu/Ta(N)/Ta(10 nm)/Si, (c) Cu/Ta(N,H)/Ta(10 nm)/Si with 5-min plasma treatment, and (d) Cu/Ta(N,H)/Ta (10 nm)/Si with 30-min plasma treatment, (e) Cu/Ta(N,O)/Ta (10 nm)/Si with 5-min plasma treatment, and (f) Cu/Ta(N,O)/Ta(10 nm)/Si with 30-min plasma treatment.

the sample with Ta barrier. In other words, nitrogen plasma treatment will restrain formation of tantalum silicide. Similar results were found for Cu/Ta(N,O)/Ta/Si annealed at 650 °C, as shown in Fig. 13(c). It is obvious that the Ta with N_2 plasma treatment possesses better thermal stability than N_2O plasma treatment. Fig. 13(d) shows the XRD spectra of Cu/Ta(N,H)/Ta/Si with NH_3 plasma treatment for 5 min before and after annealing at temperatures, 550 °C, 635 °C and 650 °C for 1 h. Strong Cu(1 1 1) and weak Cu(2 0 0) peaks are also observed in the as-deposited samples, which indicates that the Cu has preferential $\langle 111 \rangle$ crystal orientations. After annealing at 635 °C, the tantalum silicides and Ta_2N were formed. It reveals that intermixing of Ta and Si between Ta and Si interface and amorphous-like Ta(N,H) was formed in crystalline Ta_2N phase. After annealing at 650 °C for 1 h, the copper silicides were formed and grain growth of Ta silicides and Ta_2N was observed. It reveals intermixing of Cu and Si occurs through the Ta(N,H)/Ta barrier film at 650 °C. The XRD spectra of Cu/Ta(N,H)/Ta/Si with NH_3 plasma treatment for 30 min are shown in Fig. 13(e). The post-treated Ta film has a polycrystalline structure after annealing at 700 °C, and grain growth is observed after annealing at high temperatures. The post-treated Ta film on a graphite substrate showed composition of $Ta_{68}N_{32}$ as demonstrated by RBS analyses, which agrees well with the coexistence of Ta_2N. Crystal growth of Cu is observed in the annealed samples and no copper silicide forms at temperatures up to 700 °C. After annealing at 750 °C for 1 h, peaks of Cu_3Si were detected. Moreover, incorporating extra interstitial nitrogen into its structural stability against crystallization, presumably the rearrangement of the lattice atoms. As incorporation of nitrogen into Ta barrier layers can increase the crystallization temperature, the effectiveness against Cu diffusion of the ultra-thin Ta barrier film can be greatly improved by increasing nitrogen content in plasma treatment.

For the Cu/barrier/junction metallization, it is known that the leakage of diodes is more sensitive to the barrier degradation than the sheet resistance of Cu films [11]. Fig. 14 illustrates the statistical distribution of leakage current density for Cu/Ta/n^+–p, Cu/Ta(N)/Ta/n^+–p, Cu/Ta(N,O)/Ta/n^+–p, and Cu/Ta(N,H)/Ta/n^+–p junction diodes with various plasma treatment annealed at various temperatures. The Cu/Ta/n^+–p junction diodes remain stable under thermal annealing at temperature up to 475 °C, but suffer degradation in electrical characteristics at 500 °C, as shown in Fig. 14(a). For the Ta films with 30-min N_2 plasma treatment (Ta(N)/Ta), the negligible difference in leakage current between the devices of annealed at 450 °C and the as-deposited devices was observed in this study, as shown in Fig. 14(b). The devices remain stable in junction leakage even annealing at 650 °C. Figs. 14(c) and (d) illustrate the statistical distribution of leakage current density for the Cu/Ta/n^+–p junction diodes with NH_3 plasma treatment of various durations. Fig. 14(c) shows the leakage current density of Cu/Ta/n^+–p junction diodes with 5-min NH_3 plasma treatment. It shows that the devices remain stable after annealing at temperature up to 600 °C. If we define a degradation criterion with 10^{-7} A/cm^2, the barrier properties of the Ta(N,H)/Ta (5-min NH_3 plasma treatment) films are not satisfactory below 625 °C for annealing of Cu/Ta(N,H)/Ta/Si metallization system. As compared to the leakage current distribution, the devices with 30-min N_2 plasma treatment possess better capability against Cu diffusion than those of 5-min NH_3 plasma treatment. For the Ta films with 30-min NH_3 plasma treatment, the device performance is further improved in leakage current as shown in Fig. 14(d). As compared to the junction diodes with Ta(N)/Ta barriers, the Ta(N,H)/Ta films yield better barrier capability against the Cu diffusion. It is distributed that NH_3 has lower decomposition energy, and it tends to decompose into hydrogen and nitrogen ions, which interact with Ta films. The higher amount of nitrogen ions and radicals will be stuffed into grain boundaries and induce the nitridation effect against copper atoms diffusion into n^+–p junction. Figs. 14(e) and (f) illustrate the statistical distribution of leakage current density for the Cu/Ta(N,O)/Ta/n^+–p junction diodes annealed at various temperatures. Cu/Ta/n^+–p junction diodes with 5-min N_2O plasma treatment remain stable under thermal annealing at temperature up to 550 °C, but suffer degradation in electrical characteristics at 600 °C, as shown in Fig. 14(c). Similar results were obtained when the electrical characteristics of Cu/Ta/n^+–p junction diodes was treated with 30-min N_2O plasma treatment. It is seen that the N_2O plasma treated Ta films improve the electrical characteristics of sputtered Ta. However, as compared with N_2 and NH_3 plasma treated Ta films, Ta barrier with NH_3 plasma treatment possesses the best barrier capability against the Cu diffusion than the others.

4. Conclusion

In the present study, the barrier capability of the reactively sputtered Ta film and Ta film with plasma treatment against Cu diffusion was investigated. It is found that as-deposited Ta film acts an effective barrier against Cu diffusion at a temperature up to 475 °C. However, when Cu/Ta/n^+–p junction diodes were annealed up to 500 °C, the devices all failed by the junction leakage evaluation. On the other hand, plasma treated Ta films as diffusion barriers will further improve the thermal stability of Cu/Ta/n^+–p junction diodes to 650 °C. The plasma treatments provide a new method of forming nitrogen incorporated Ta films with low resistivity, small grain sizes, and high thermal stability. It is attributed to nanocrystallization and stuffing effect due to plasma treatment. NH_3 plasma treated Ta film possesses the best thermal stability than all the others. Excited species produced in the plasma enhanced the nitridation reaction and the oxygen/nitrogen exchange, which allows complete nitridation of the thin layer on tantalum film. Hydrogen species produced in the NH_3 plasma are

thought to play a major role in the enhancement of eliminating oxygen contents from the film. Furthermore, by plasma nitridation, the enhancement of the barrier performance will be able to alleviate copper diffusion into Si substrate.

Acknowledgements

The work was financially supported by the National Science Council of the Republic of China under Contract No. NSC-93-2320-B-038-034 and this study was sponsored by Taipei Medical University Hospital (TMU92-AE1-B02).

References

[1] T. Nitta, T. Hoshi, S. Sakai, K. Sakaibara, S. Imai, T. Shibata, J. Electrochem. Soc. 140 (1993) 1131.
[2] Y.J. Lee, B.S. Suh, M.S. Kwon, C.O. Park, J. Appl. Phys. 85 (1999) 1927.
[3] M.J. Attardo, R. Rosenberg, J. Appl. Phys. 41 (1970) 2381.
[4] L. Stolt, F.M. d'Heurle, Thin Solid Films 189 (1990) 269.
[5] M.-A. Nicolet, Thin Solid Films 52 (1978) 415.
[6] R.S. Nowicki, M.-A. Nicolet, Thin Solid Films 96 (1982) 317.
[7] M. Wittmer, J. Vac. Sci. Tech. A. 2 (1984) 273.
[8] J.O. Olowolafe, J. Li, B. Blanpain, J.W. Mayer, Appl. Phys. Lett. 57 (1990).
[9] B.S. Suh, Y.J. Lee, J.S. Hwang, C.O. Park, Thin Solid Films 348 (1999) 299.
[10] W.F. Wu, K.L. Ou, C.P. Chou, J.L. Hsu, Electrochem. Solid-State Lett. 6 (2) (2003) G27.
[11] W.L. Yang, W.F. Wu, D.G. Lin, C.C. Wu, K.L. Ou, Solid-State Electron. 45 (2001) 149.
[12] X. Sun, E. Kolawa, J.S. Chen, J.S. Reid, M.A. Nicolet, Thin Solid Films 236 (1993) 347.
[13] K.M. Chang, T.H. Yeh, I.C. Deng, C.W. Shih, J. Appl. Phys. 82 (1998) 2538.
[14] S.S. Wang, C. Ryu, H. Lee, L.S. Loke, K.W. Kwon, S. Bhattacharya, R. Eaton, R. Faust, B. Mikkola, J. Mucha, J. Ormando, IITC 107 (1998).
[15] K.L. Ou, W.F. Wu, C.P. Chou, C.S. Chiou, C.C. Wu, J. Vac. Sci. Tech. B. 20 (5) (2002) 2154.
[16] K.L. Ou, Microelectro. Eng. 83 (2) (2006) 312.
[17] K.L. Ou, Ming-Sun Yu, R.Q. Hsu, M.H. Lin, J. Vac. Sci. Tech. B. 23 (1) (2005) 229.
[18] K.L. Ou, M.H. Tsai, H.M. Huang, S.Y. Chiou, C.T. Lin, S.Y. Lee, Microelectro. Eng. 77 (2) (2005) 184.
[19] H. Kim, C. Cabral Jr., C. Lavoie, S.M. Rossnagel, J. Vac. Sci. Tech. B. 20 (4) (2002) 1321.
[20] X.P. Qu, M. Zhou, T. Chen, Q. Xie, G.P. Ru, B.Z. Li, Microelectro. Eng. 83 (2006) 236.